

# Exchange interactions, spin waves, and Curie temperature in zincblende half-metallic sp-electron ferromagnets: the case of CaZ (Z = N, P, As, Sb)

A Laref<sup>1,2</sup>, E Şaşıoğlu<sup>3,4</sup> and I Galanakis<sup>5</sup>

<sup>1</sup> Department of Physics, Pohang University of Science and Technology, Pohang 790-784, Korea

<sup>2</sup> Max-Planck-Institut für Mikrostrukturphysik, Weinberg 2, D-06120 Halle, Germany

<sup>3</sup> Peter Grünberg Institut and Institute for Advanced Simulation, Forschungszentrum Jülich and JARA, 52425 Jülich, Germany

<sup>4</sup> Department of Physics, Fatih University, 34500, Büyükçekmece, İstanbul, Turkey

<sup>5</sup> Department of Materials Science, School of Natural Sciences, University of Patras, Patras 26504, Greece

E-mail: [larefamel@yahoo.com](mailto:larefamel@yahoo.com), [e.sasioglu@fz-juelich.de](mailto:e.sasioglu@fz-juelich.de) and [galanakis@upatras.gr](mailto:galanakis@upatras.gr)

Received 6 April 2011, in final form 8 June 2011

Published 27 June 2011

Online at [stacks.iop.org/JPhysCM/23/296001](http://stacks.iop.org/JPhysCM/23/296001)

## Abstract

Using first-principle calculations in conjunction with the frozen-magnon technique we have calculated the exchange interactions and spin-wave dispersions in the series of the zincblende half-metallic II–V (CaZ, Z = N, P, As, Sb) ferromagnets. The calculated exchange constants are used to estimate the Curie temperature within the random phase approximation. The large Stoner gap in these alloys gives rise to well-defined undamped spin waves throughout the Brillouin zone. Moreover we show that the spin-wave stiffness constants for the considered systems are among the largest available for local moment ferromagnets. The predicted Curie temperature of half-metallic CaN is noticeably higher than the room temperature with respect to the other compounds, and thus we propose CaN as a promising candidate for future applications in spintronic devices.

(Some figures in this article are in colour only in the electronic version)

## 1. Introduction

Since the discovery of half-metallic ferromagnetism in CrAs when grown as thin film in the metastable zincblende structure using the molecular beam epitaxy technique by Akinaga *et al* [1], a lot of interest has been focused on the study of similar pnictides and chalcogenides (for a review on these alloys see [2] and for a wider review on half-metals see [3]) due to their potential applications in spintronic devices and their coherent growth on top of binary semiconductors with the same lattice structure. Although the interest has mainly focused on the compounds containing transition metal atoms, several theoretical studies have been also devoted to the so-called sp-electron ferromagnets. Unfortunately, contrary to transition

metal pnictides, the sp-electron ferromagnets have not yet been synthesized experimentally. In 2003 Geshi *et al* were the first to predict using first-principles calculations that CaP, CaAs and CaSb compounds in the zincblende structure are half-metallic ferromagnets, i.e. one spin band is metallic while the other is semiconducting [4]. In the following year Kusakabe *et al* focused on the CaAs alloy and found that ferromagnetism is due to a flat band created by the hybridization of the localized Ca d and As p-states [5]; the p orbitals transform using the same symmetry group with the  $t_{2g}$  d orbitals and thus can hybridize. Following these two pioneering papers a lot of effort has been devoted to the study of sp-electron ferromagnets in several lattice structures. Sieberer and collaborators studied all possible II–V combinations in the zincblende (zb) structure

**Table 1.** Lattice parameter  $a$  in Å used in the calculations (CaN is taken from [6] and the rest from [4]), atom  $m_i$  and total  $m_{\text{cell}}$  spin magnetic moments in  $\mu_B$ , Stoner gap  $\Delta S$  in eV and spin-wave stiffness constant  $D$  in  $\text{meV \AA}^2$  for the CaZ ( $Z = \text{N, P, As, Sb}$ ) compounds.

	$a$	$m_{\text{Ca}}$	$m_Z$	$m_{\text{Void1}}$	$m_{\text{Void2}}$	$m_{\text{cell}}$	$\Delta S$	$D$
CaN	5.47	0.04	0.98	0.01	-0.03	1.00	0.76	790
CaP	6.55	0.12	0.85	0.04	-0.01	1.00	0.54	1268
CaAs	6.75	0.15	0.81	0.05	-0.01	1.00	0.44	1420
CaSb	7.22	0.19	0.77	0.03	0.01	1.00	0.30	1554

and found that ferromagnetism exists for large unit cell volumes [6]; Yao and collaborators expanded this study to cover also the case where the V-column element is Bi [7]. Volnianska and Boguslawski have also considered the case of rocksalt, NiAs and  $\text{Zn}_3\text{P}_2$  structures, and have shown that the rocksalt structure is the most stable while spin polarization is more stable for nitrides [8]. Similar work by Gao *et al* has confirmed that only nitrides retain the half-metallic character in the rocksalt structure [9]. Gao and collaborators also studied the case of II–VI zincblende compounds where the VI-column element is C, Si or Ge [10–12] while a study of SrC also in the wurtzite structure exists in the literature [13]. Li and Yu in 2008 have shown that the inclusion of spin-orbit coupling destroys the half-metallic character in the case of zincblende Ca(As, Sb, Bi) alloys but not for the lighter CaN and CaP compounds [14]. The surface properties of CaC [15], and the properties of surfaces and interfaces with binary semiconductors of the Ca and Sr nitrides [16] have also been studied. Finally the case of I–V compounds (Li, Na, K) (N, P, As) has been studied and nitrides have also been found to be half-metallic ferromagnets [17].

Although the electronic properties and the spin magnetic moments of the half-metallic sp-electron ferromagnets have been studied in great detail, the stability of ferromagnetism via the calculation of exchange constants has been explored only in the case of carbonides. In [12] the exchange constants for rocksalt SrC and BaC have been calculated using the frozen-magnon approximation, and in [10] similar calculations have been performed for the zb CaC, SrC and BaC alloys. The leading interactions are between the carbon atoms which mainly carry the magnetic moments. Estimated Curie temperatures were found to be higher for the compounds in the zb structure and CaC exhibited the highest one, reaching 735 K within the random phase approximation (RPA). The scope of our present study is to explore the magnetic properties such as exchange constants, Curie temperatures and spin waves for the zb CaZ ( $Z = \text{N, P, As, Sb}$ ) alloys, which are the most studied ones, and since, as mentioned above, the CaN and CaP retain their half-metallic character even when spin-orbit coupling is taken into account [14]. These properties are directly related to the robustness of ferromagnetism and thus are relevant to any potential applications of these alloys. To perform this study we use the same methodology as for the zb transition metal pnictides and chalcogenides used in [18]. In section 2 we will provide details about the method which we adopt, in section 3 we will analyze our results and finally in section 4 we will summarize our results and present our conclusions.

## 2. Method

The ground-state electronic structure calculations are carried out using the augmented spherical waves method (ASW) [19] within the atomic-sphere approximation (ASA) [20]. In the zb lattice two empty spheres are used to account for the empty sites. The exchange–correlation potential is chosen in the generalized gradient approximation [21]. A dense Brillouin zone sampling  $30 \times 30 \times 30$  is used. The radii of all atomic spheres are chosen equal. For our calculations we have used the optimized lattice constants from [4] which are almost identical to the equilibrium lattice constants calculated in [6] (for CaN we used the value from [6]), and we present them in table 1.

Before presenting the key points of our method to calculate the exchange constants we should briefly first discuss excitations in these alloys. There two kind of magnetic excitations: (i) Stoner type and (ii) magnons. The Stoner excitations involve excitations from the occupied majority-spin states to the unoccupied minority-spin states and thus are affected by the exchange splitting of the bands [22]. Even in usual metals they correspond to high excitation energies and in systems like the ones studied here, where a gap exists in the minority-spin gap and exchange splitting is very strong, they can be neglected even when the Curie temperature is calculated, as shown by Edwards and Katsnelson in the case of sp-impurity bands in  $\text{CaB}_6$  [23]. An estimation of the energy position of these excitations is given by the so-called Stoner gap  $\Delta S$  which is the energy difference between the highest occupied majority-spin state and the lowest unoccupied minority-spin state, and thus corresponds to the lowest possible Stoner excitation energy [22]. We present the calculated values from our density of states (DOS) data in table 1 for all four compounds under study and, as shown, the values vary between 0.30 eV for CaSb and 0.76 eV for CaN and thus Stoner excitations can be neglected in the discussion of thermodynamic properties [23].

The second kind of excitations are the so-called ‘magnons’ which involve collective excitations of the spin magnetic moments. In a simplified picture we can assume that the magnitude of the spin magnetic moments of the atoms does not change with respect to the 0 K value calculated using *ab initio* electronic structure methods. However, as we raise the temperature atomic spin moments change their orientation in such a way that the azimuthal angle can be described by a propagating plane wave characterized by a vector  $\mathbf{q}$  belonging in the Brillouin zone. This is the so-called spin wave or magnon. If the magnitude of  $\mathbf{q}$  is small we can assume that the energy for the creation of the spin wave is given by the relation  $E(\mathbf{q}) = D|\mathbf{q}|^2$  and thus depends only on the

magnitude of the wavevector, and not its orientation in the Brillouin zone; this usually occurs around the  $\Gamma$  point as we will show later on when presenting the energy dispersion of the spin waves. The constant  $D$  is referred to as the ‘spin-wave stiffness constant’ and we present its calculated value in table 1. In transition metal ferromagnets like Fe, Co and Ni the value of  $D$  is about 300–600 meV  $\text{\AA}^2$  (see table 2 in [24]) and the largest known values are 715 meV  $\text{\AA}^2$  for  $\text{Co}_2\text{FeSi}$  [25] and 800 meV  $\text{\AA}^2$  for  $\text{Fe}_{53}\text{Co}_{47}$  [26]. But as shown in table 1 and discussed in section 3, for the compounds under study it surpasses these values ranging from 790 meV  $\text{\AA}^2$  for CaN up to 1554 meV  $\text{\AA}^2$  for CaSb. Magnons dominate the lower part of the excitation spectra and especially for the systems under study here and, as shown by the spin-wave dispersion energies discussed in section 3, they are separated by a gap from the Stoner excitations. Thus the consideration only of magnons is justified for the calculation of the thermodynamic properties of calcium pnictides.

Electronic structure results are used to estimate the exchange constants within the frozen-magnon approximation [27]. The method of the calculation of the exchange constants within the frozen-magnon approximation has already been presented elsewhere [28]. Here, to make the paper reasonably self-contained, a brief overview is given. Notice that since the magnetism is almost exclusively concentrated on the  $Z = \text{N, P, As or Sb}$  atoms and the Ca–Ca intrasublattice and Ca– $Z$  intersublattice interactions are negligible, as confirmed also from our calculations, the equations presented below are for systems with only one magnetic sublattice for reasons of simplicity. It should be noted that the frozen-magnon technique does not allow us to access spin-wave lifetimes since it is a static approximation. The lifetimes can be obtained from dynamical spin susceptibility calculations within time-dependent density functional theory (TDDFT) [29] or many-body perturbation theory [30]. In magnetic materials with a Stoner gap larger than the spin-wave energies such as half-metals or semiconductors the spin waves exist throughout the Brillouin zone and are not damped. Thus, the frozen-magnon method and TDDFT give practically the same results for the spin-wave dispersion as shown in [29] for the case of NiMnSb, which has also a large Stoner gap.

To calculate the interatomic exchange interactions we use the frozen-magnon technique [27] and map the results of the calculation of the total energy of the helical magnetic configurations

$$\mathbf{s}_n = (\cos(\mathbf{q}\mathbf{R}_n) \sin \theta, \sin(\mathbf{q}\mathbf{R}_n) \sin \theta, \cos \theta) \quad (1)$$

onto a classical Heisenberg Hamiltonian

$$H_{\text{eff}} = - \sum_{i \neq j} J_{ij} \mathbf{s}_i \cdot \mathbf{s}_j \quad (2)$$

where  $J_{ij}$  is an exchange interaction between two  $Z$  sites and  $\mathbf{s}_i$  is the unit vector pointing in the direction of the magnetic moment at site  $i$ .  $\mathbf{R}_n$  are the lattice vectors,  $\mathbf{q}$  is the wavevector of the helix, and  $\theta$  the polar angle giving the deviation of the moments from the  $z$  axis. Within the Heisenberg model (2), the

energy of frozen-magnon configurations can be represented in the form

$$E(\theta, \mathbf{q}) = E_0(\theta) - \sin^2 \theta J(\mathbf{q}) \quad (3)$$

where  $E_0$  does not depend on  $\mathbf{q}$  and  $J(\mathbf{q})$  is the Fourier transform of the parameters of exchange interaction between pairs of N (P, As or Sb) atoms:

$$J(\mathbf{q}) = \sum_{\mathbf{R}} J_{0\mathbf{R}} \exp(i\mathbf{q} \cdot \mathbf{R}). \quad (4)$$

Calculating  $E(\theta, \mathbf{q})$  for a regular  $\mathbf{q}$ -mesh in the Brillouin zone of the crystal and performing back Fourier transformation, one obtains exchange parameters  $J_{0\mathbf{R}}$  between pairs of  $Z = \text{N, P, As or Sb}$  atoms.

Regarding the Curie temperature, we employ the RPA and the Curie temperature is given by the relation [24]

$$\frac{1}{k_B T_C^{\text{RPA}}} = \frac{6\mu_B}{M} \frac{1}{N} \sum_q \frac{1}{\omega(\mathbf{q})}, \quad (5)$$

where  $\omega(\mathbf{q}) = \frac{4}{M}[J(0) - J(\mathbf{q})]$  is the energy of spin-wave excitations,  $\mu_B$  is the Bohr magneton,  $M$  is the magnitude of the atomic spin magnetic moments and the sum runs over the  $N$  values of the  $\mathbf{q}$ -wavevector considered in the Brillouin zone. RPA formalism takes into account only transverse spin fluctuations (magnons) and the single-particle spin-flip excitations (Stoner excitations) are neglected. Thus its use is well grounded for the alloys under study here since, as we discussed above, the latter ones play no practical role in the thermodynamics of the systems of interest in our study. We have not employed the mean-field approximation (MFA) since the latter corresponds to an equal weighting of the low- and high-energy spin-wave excitations, leading to an overestimation of the experimental Curie temperature contrary to RPA where the lower-energy excitations make a larger contribution to the Curie temperature leading to more realistic values [24, 31, 32].

### 3. Results and discussion

We will start our discussion from the electronic properties of the compounds under study. As mentioned above we have used the equilibrium lattice constants from [6] for CaN and from [4] for the other three compounds. In table 1 we gather the values of the lattice constants which vary from 5.47  $\text{\AA}$  for CaN up to 7.22  $\text{\AA}$  for CaSb. We should note here that contrary to the other three compounds, CaN’s lattice constant is close to the values of several zb binary semiconductors (GaP has a lattice constant of about 5.45  $\text{\AA}$  and GaAs of 5.65  $\text{\AA}$ ) and thus coherent growth should be more likely to occur for this alloy due to the smaller strains imposed by the substrate. The reason for the large equilibrium lattice constants is the high ionicity of the calcium pnictides. As shown by Volnianska and Boguslawski due to the very high ionicity presented by these alloys they prefer to crystallize in structures with higher coordination number, like the rocksalt one, to minimize electrostatic energy and only for very large unit cell volumes does the zincblende structure become stable [8]. But as shown by Kusakabe *et al*

in the  $zb$  lattice structure, the magnetism comes from a flat band mechanism [5] and not from mechanisms like the p–d hybridization and the double-exchange usually occurring in ferromagnets containing transition metal atoms. Thus these compounds can be considered as prototype systems to study the occurrence of this mechanism.

In figure 1 we present the total density of states (DOS) together with the anionic projected one. The half-metallic gap occurs in the majority-spin band contrary to the usual half-metallic pnictides containing transition metal atoms like CrAs etc [2]. There is also a gap in the minority-spin band and the Fermi level falls within a peak of the minority-spin DOS. Notice also that the states below the gaps in both spin directions are almost exclusively of anionic character (N, P, As or Sb) while the bands above the gaps are of cationic character (Ca). Also, the width of the gaps is unusually large and the tendency as we move along the Vth column from N to Sb is the decrease of the gap width followed by smaller band widths. This behavior can be traced to the band structure [5]. Each Ca atom provides two electrons which occupy the 4s-states in the free atom, while each anion provides in total five electrons: two occupying the valence s-states and three the valence p-states in the free atom. Thus in total we have seven valence electrons. The anions create an s-band deep in energy, not shown here, which accommodates two valence electrons. The p-states of the anions can hybridize exclusively with the  $t_{2g}$  d-states of Ca, which transform following the same symmetry group. However, these states are high in energy above the gaps for both spin directions, and thus the weight of the bands below the gaps is mainly of anionic p-character. The small Ca d-admixture in the occupied states is due to the fact that anionic p-states are extended in space and, if we express the wavefunctions within a sphere centered at the cationic center and use as point of origin the cationic site, then  $t_{2g}$  d-states appear in the expression of the wavefunctions since they are the only ones compatible with respect to their symmetry. This d-admixture plays a crucial role since it leads to an almost dispersionless flat p-band exactly at the top of the other two p bands, as shown by Kusakabe *et al* [5]. The splitting of the flat bands of different spin character leads to the complete occupation of the one in the majority-spin band and to an empty flat band in the minority-spin band. Thus the majority-spin p bands contain three electrons and the minority-ones two electrons. The Ca atoms also play a second decisive role in the appearance of half-metallicity since they provide two valence electrons which, due to the high-energy position of the Ca 4s-states in the crystal, occupy the p-states offered by the anionic atom. The difference in the width of the gaps and the bands should be mainly attributed to the large variation of the lattice constants as we move from CaN to CaSb. Large unit cell volumes mean less hybridization and more atomic-like behavior of the p-states and thus more narrow bands and smaller gaps.

We should also discuss the spin magnetic moments presented in table 1. As discussed above, we have also used two empty sites (Void1 and Void2) to account correctly for the empty space in the  $zb$  structure. In table 1 we have also included the spin magnetic moments at these two sites,

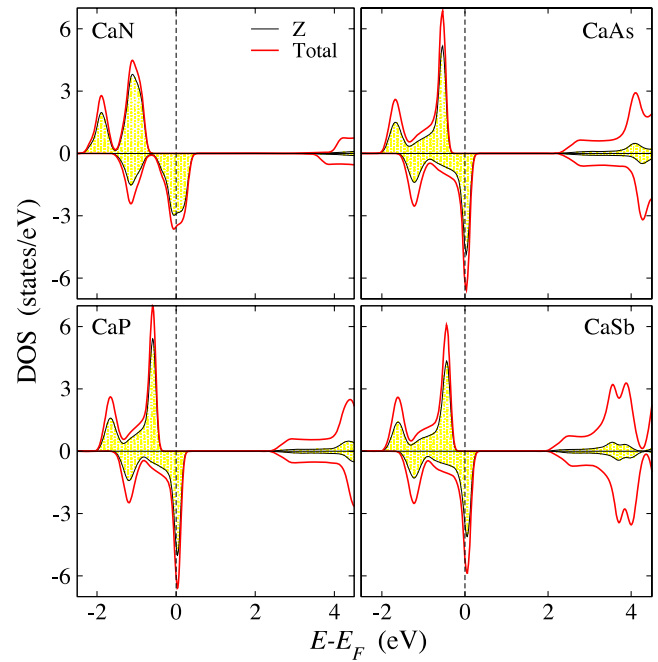


**Figure 1.** Total density of states (DOS) and its projection on the anionic atom (N, P, As, Sb) for the CaZ compounds. We have set the Fermi level as the zero of the energy axis. Note that positive values of DOS refer to the majority-spin electrons and negative values to the minority-spin electrons.

but since the charge in the two voids is very small the spin moments are also negligible. As expected from the discussion on the DOSs, the magnetic moments are mainly carried by the anions. Especially for CaN, where N is the lighter element, the contribution of Ca to the total spin moment can be safely neglected. As we move from CaN to CaSb the spin moment at the anionic sites decreases and it is counterbalanced by an increase of the spin moment at the Ca site which reaches a value of  $0.19 \mu_B$  for CaSb. The observed trend is expected since the spin splitting for the valence 5p-states of the heavy Sb atom is more difficult to achieve than for the valence 2p states of the light N atom. In all cases the total spin magnetic moment is exactly  $1 \mu_B$ . In the zincblende alloys like the ones under study, irrespective of whether or not they contain transition metal atoms, we have exactly four states below the half-metallic gap: one s-like and three p–d ones (in the sp-electron ferromagnets under study the p-character dominates with respect to the transition metal ones [33]). Thus the total spin magnetic moment in  $\mu_B$  follows a Slater–Pauling behavior and should be  $|8 - Z_t|$ , where  $Z_t$  is the total number of valence electrons in the unit cell. Here Ca contributes two valence electrons and the anionic atoms five, and thus in total we have seven valence electrons and from the just-mentioned rule the total spin magnetic moment should be  $1 \mu_B$ , as confirmed by our electronic structure calculations.

Since the magnetic moments are mainly concentrated at the anionic atoms we expect that their interaction is the most relevant for the discussion of the stability of ferromagnetism. Indeed our calculations show that the Ca–Ca intrasublattice and Ca–N (P, As, Sb) intersublattice interactions have a negligible contribution to the exchange constants, and thus

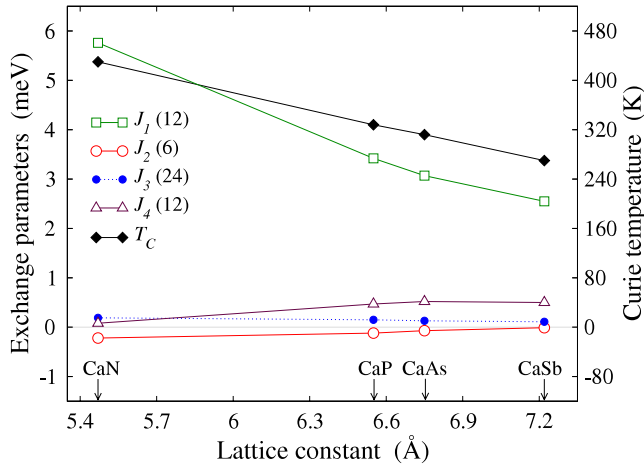


**Figure 2.** The effective Z–Z ( $Z = \text{N, P, As, Sb}$ )  $J_i$  ( $i = 1-4$ ) exchange interaction constants and the RPA-calculated Curie temperature as a function of their corresponding lattice spacing. In parenthesis is the number of neighbors within the  $i$ th coordination shell. The Ca–Ca intrasublattice and Ca–Z intersublattice constants are almost vanishing and thus are not presented.

we do not present them here. Moreover as we discussed in section 2 and as deduced from the values of the Stoner gaps (minimum energy required for such an excitation) presented in table 1 the Stoner excitations, which involve excitation from the occupied majority-spin states to the unoccupied minority-spin states, occur at the high-energy region of the excitation spectra and can be neglected [23]. The Z–Z intrasublattice exchange constant within the frozen-magnon approximation discussed in section 2 is presented in figure 2. The index refers to the Z–Z coordination shell. We present results up to the fourth coordination shell. The first remark is that only the interactions between nearest anionic Z atoms  $J_1$  play an important role since contributions from other coordination shells are almost vanishing. Each Z atom has 12 nearest Z atoms which in reality are second-neighbors (each Z atom has as nearest-neighbors eight Ca atoms). The  $J_1$  has a value ranging from about 6 meV for CaN down to 2.5 meV for CaSb. The value for CaN is high enough to lead to stable ferromagnetic order and a Curie temperature well above the room temperature as we will also discuss later. The value of  $J_1$  is much larger for the lighter N atom due to the larger anionic spin magnetic moment in CaN and the much smaller N–N spacing in CaN with respect to the other three compounds under study. Here we should note that, for zb half-metallic CaC studied in [10] the value of  $J_1$  characterizing the C–C interactions was 0.906 mRyd, which equals 12.33 meV, double the N–N values due to the much larger C spin magnetic moment; C has one electron less than N and due to the Slater–Pauling rule CaC has a total spin magnetic moment of  $2 \mu_B$  carried mainly by the carbon atoms. Finally we should note that in the case of transition metal zb-pnictides like CrAs the Cr–Cr  $J_1$  value is even larger reaching 18 meV, triple the N–N value, due to the even larger Cr spin magnetic moment of about  $3 \mu_B$  [18]. Thus the flat band mechanism can lead to stable ferromagnetism as for CaN and the values of the exchange constants depend mainly on the values of the spin magnetic

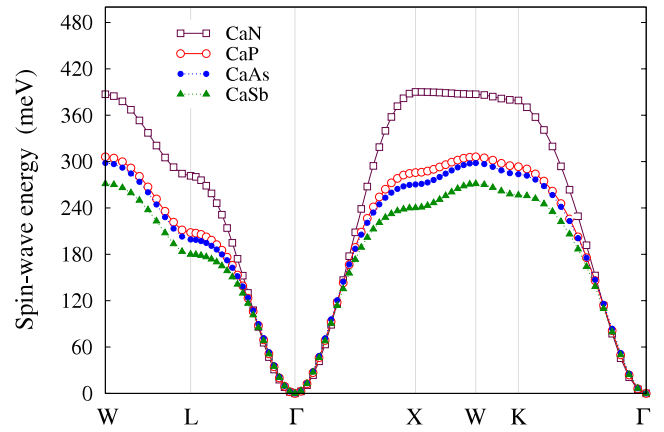


**Figure 3.** The spin-wave dispersion along the high-symmetry lines in the Brillouin zone for the CaZ compounds where Z is N, P, As and Sb.

moments and not on the underlying mechanism responsible for the appearance of ferromagnetism.

We will conclude our study with a discussion about the Curie temperatures,  $T_C$ , in the CaZ alloys. As we mentioned in section 2 we employ the random phase approximation (RPA) in which low-energy excitations have a larger weight on the estimated  $T_C$  with respect to the high-energy excitations. Moreover the stronger the ferromagnetism the larger should be the value of the estimated  $T_C$ . As we will show, the values which we have calculated are compatible with this picture. In figure 2 we present the RPA-calculated values of the Curie temperature. As expected, trends follow the trend of the  $J_1$  exchange constants. For CaN  $T_C$  is 430 K well above room temperature, for CaP and CaAs it is close to room temperature (350 K and 290 K respectively) and for CaSb it is 280 K, being below room temperature. Note that zb CaC has an RPA estimated  $T_C$  of 735 K [10] and the RPA  $T_C$  of zb CrAs exceeds the 1000 K [18] following the trends of  $J_1$  discussed in the previous paragraph. Thus for realistic applications only CaN seems to be appealing. The curve followed by the Curie temperature in figure 2 does not exactly have the same gradient as the curve for the  $J_1$  since also further neighbor exchange constants contribute to  $T_C$  and as we can see in the figure  $J_{2,3,4}$  have an almost zero value for CaN but small positive values for the other three alloys (although their values stay extremely small compared to  $J_1$ ). Finally the higher  $T_C$  value for CaN with respect to the other three alloys can be also deduced using as the starting point the energies of the spin waves. As shown in equation (5), the  $\frac{1}{T_C}$  is directly proportional to the sum over the whole Brillouin zone of the  $\frac{1}{\omega(\mathbf{q})}$  where  $\omega(\mathbf{q})$  is the spin-wave dispersion energy; we present these for all four compounds under study in figure 3 along the high-symmetry lines in the Brillouin zone. We can see that the dispersion curve for CaN is for all  $\mathbf{q}$ -points well above the curves for the other three compounds especially along the X–W–K lines where it makes also a high-energy plateau. Thus the sum which we just mentioned is much smaller for CaN and the Curie temperature which is the inverse of the sum is much larger. As we move along the Vth column in the periodic table from

N to P and then to As and finally to Sb the dispersion energies for the same  $\mathbf{q}$  are lower, leading to smaller estimated Curie temperatures. It should be noted that, in contrast to metals, in the present compounds well-defined undamped spin waves exist throughout the Brillouin zone [29]. This stems from the large Stoner gaps (see table 1), which separate single-particle spin-flip Stoner excitations from the collective spin waves (see figure 3). Around the  $\Gamma$  point ( $\mathbf{q} = 0$ ), as we also discussed in section 2, we can state that the magnitude of the wavevector is small and the energy for the creation of the spin wave can be approximated by the relation  $E(q) = D|q|^2$ , where  $D$  is the spin-wave stiffness constant and  $q$  is the magnitude of the wavevector  $\mathbf{q}$  in units of  $\frac{2\pi}{a}$  where  $a$  is the lattice constant. We present the values of  $D$  in table 1. Its value ranges from 790 meV  $\text{\AA}^2$  for CaN to 1554 meV  $\text{\AA}^2$  for CaSb, these being among the largest known values in the literature as discussed in section 2. Thus for the same  $\mathbf{q}$ , when we are close to the  $\Gamma$  point, the dispersion energy is almost double for CaSb with respect to CaN but this occurs only in a very limited region around the  $\Gamma$ -point and its effect is washed out from the influence on the  $T_C$  of the rest of the Brillouin zone where the dispersion energy for the same  $\mathbf{q}$  is much larger for CaN than CaSb. Thus the calculation of the spin-wave stiffness constant is not a reliable indication for the behavior of the Curie temperature

#### 4. Conclusions

In summary, we have calculated from first-principles the electronic structure and employed the frozen-magnon approximation to evaluate the exchange parameters in zincblende calcium pnictides, which are prototypes for the appearance of flat band sp-electron ferromagnetism. We have also determined the spin-wave dispersion energies, spin-wave stiffness constants and Curie temperatures of the considered systems on the same footing, namely, all based on calculated values of exchange parameters. All compounds are half-metallic with the gap in the majority-spin band contrary to transition metal zincblende pnictides. Calculation of the exchange constants shows that interaction between nearest anionic atoms (N, P, As or Sb) is the dominant one, and its value for CaN is double that for the other three compounds under study, leading also for CaN to a Curie temperature above room temperature. Calculated spin-wave stiffness constants are the largest known for intermetallic compounds. Although CaSb exhibits the largest value, the situation is the inverse when we look at the spin-wave energy dispersion in the whole Brillouin zone in agreement with the higher Curie temperature exhibited by the CaN compound.

We conclude that CaN possesses properties which make it a promising candidate for spintronic applications: small lattice constant, large half-metallic gap and high Curie temperature. It is hoped that our results would motivate further theoretical and experimental research in this field. We expect that the present study will stimulate experimental efforts toward the possible growth of zincblende CaN thin films or multilayers on suitable substrates using modern deposition techniques, e.g. pulsed laser deposition and molecular beam epitaxy.

#### Acknowledgment

Fruitful discussions with L M Sandratskii are gratefully acknowledged.

#### References

- [1] Akinaga H, Manago T and Shirai M 2000 *Japan. J. Appl. Phys.* **39** L1118
- [2] Mavropoulos Ph and Galanakis I 2007 *J. Phys.: Condens. Matter* **19** 315221
- [3] Katsnelson M I, Irkhin V Yu, Chioncel L, Lichtenstein A I and de Groot R A 2008 *Rev. Mod. Phys.* **80** 315
- [4] Geshi M, Kusakabe K, Tsukamoto H and Suzuki N 2004 arXiv:cond-mat/0402641
- [5] Kusakabe K, Geshi M, Tsukamoto H and Suzuki N 2004 *J. Phys.: Condens. Matter* **16** S5639
- [6] Sieberer M, Redinger J, Khmelevskiy S and Mohn P 2006 *Phys. Rev. B* **73** 024404
- [7] Yao K L, Jiang J L, Liu Z L and Gao G Y 2006 *Phys. Lett. A* **359** 326
- [8] Volnianska O and Boguslawski P 2007 *Phys. Rev. B* **75** 224418
- [9] Gao G Y, Yao K L, Liu Z L, Zhang J, Min Y and Fan S W 2008 *Phys. Lett. A* **372** 1512
- [10] Gao G Y, Yao K L, Şaşıoğlu E, Sandratskii L M, Liu Z L and Jiang J L 2007 *Phys. Rev. B* **75** 174442
- [11] Gao G Y, Yao K L, Liu Z L, Jiang J L, Yu L H and Shi Y L 2007 *J. Phys.: Condens. Matter* **19** 315222
- [12] Gao G Y and Yao K L 2007 *Appl. Phys. Lett.* **91** 082512
- [13] Zhang C-W, Yan S-S and Li H 2008 *Phys. Status Solidi b* **245** 201
- [14] Li Y and Yu J 2008 *Phys. Rev. B* **78** 165203
- [15] Gao G Y, Yao K L and Li N 2011 *J. Phys.: Condens. Matter* **23** 075501
- [16] Gao G Y, Yao K L, Liu Z L, Min Y, Zhang J, Fan S W and Zhang D H 2009 *J. Phys.: Condens. Matter* **21** 275502
- [17] Gao G Y and Yao K-L 2009 *J. Appl. Phys.* **106** 053703
- [18] Şaşıoğlu E, Galanakis I, Sandratskii L M and Bruno P 2005 *J. Phys.: Condens. Matter* **17** 3915
- [19] Williams A R, Kübler J and Gelatt C D 1979 *Phys. Rev. B* **19** 6094
- [20] Andersen O K 1975 *Phys. Rev. B* **12** 3060
- [21] Perdew J P and Wang Y 1992 *Phys. Rev. B* **45** 13244
- [22] Glazer J and Tosatti E 1984 *Solid State Commun.* **52** 905
- [23] Edwards D M and Katsnelson M I 2006 *J. Phys.: Condens. Matter* **18** 7209
- [24] Pajda M, Kudrnovsky J, Turek I, Drchal V and Bruno P 2001 *Phys. Rev. B* **64** 174402
- [25] Gaier O, Hamrle J, Trudel S, Hillebrands B, Schneider H and Jakob G 2009 *J. Phys. D: Appl. Phys.* **42** 232001
- [26] Liu X, Sooryakumar R, Gutierrez C J and Prinz G A 1994 *J. Appl. Phys.* **75** 7021
- [27] Sandratskii L M and Bruno P 2002 *Phys. Rev. B* **66** 134435
- [28] Şaşıoğlu E, Sandratskii L M and Bruno P 2004 *Phys. Rev. B* **70** 024427
- [29] Buczek P, Ernst A, Bruno P and Sandratskii L M 2009 *Phys. Rev. Lett.* **102** 247206
- [30] Şaşıoğlu E, Schindlmayr A, Friedrich C, Freimuth F and Blügel S 2010 *Phys. Rev. B* **81** 054434
- [31] Şaşıoğlu E, Sandratskii L M, Bruno P and Galanakis I 2005 *Phys. Rev. B* **72** 184415
- [32] Şaşıoğlu E, Sandratskii L M and Bruno P 2005 *J. Appl. Phys.* **98** 063523
- [33] Galanakis I and Mavropoulos Ph 2003 *Phys. Rev. B* **67** 104417